Seismic Hazard Assessment of a Residential Building in Metro Manila using Reliability-based Methods

Engr. Cesar P. Malenab Jr.

ABSTRACT: Statistics of significant earthquakes ($M_w \geq 5.0$ and distance ≤ 400 km) are presented for a residential building in Metro Manila based on an earthquake catalog in the past 122 years. Seismic assessment utilizing conventional Probabilistic Seismic Hazard Analysis (PSHA) is verified using reliability-based methods by comparing the uniform hazard spectra (UHS). The analysis shows that the reliability-based approach overestimates the spectral accelerations at a period range of 0 to 0.15s while underestimating at a period range of 0.15 to 5s. PGA, S_s, and S_1 from the simulation are within the Philippine Earthquake Model (PEM) recommendations. The study shows that reliability-based methods can be an alternative approach to seismic hazard assessment since the two methods are mutually confirmatory.

KEYWORDS: *PSHA; Reliability Methods; Uniform hazard spectrum; Philippine Earthquake Model*

I. INTRODUCTION

Prediction of ground motion intensities of different hazard levels is essential, especially in highly urbanized areas like Metro Manila. In this regard, seismic hazard assessments are conducted to aid structural engineers in designing earthquake-resistant structures and ensure that structures are within a desired level of performance. Probabilistic Seismic Hazard Analysis (PSHA) is a mathematical approach that accounts for the stochastic nature of earthquakes and gives the future ground motions that may occur at a given site. PSHA is composed of five steps (Baker, 2015): (1) identification of sources of potentially damaging earthquakes, (2) characterization of the distribution of earthquake magnitudes, (3) characterization of source-to-site distances of potential earthquakes, (4) prediction of the resulting ground motion intensity, and (5) combining uncertainties in earthquake size, location, and intensity using the total probability theorem. The recent release of the Philippine Earthquake Model (PEM) and Spectral Acceleration Maps of the Philippines (SAM-PH) based on the probabilistic seismic hazard analysis will be adapted as the new seismic design approach for the next issue of the National Structural Code of the Philippines (NSCP). It will serve as the minimum design requirements for the design of structures.

From a different perspective, Musson (2012) pointed out that the results of PSHA using the Cornell-McGuire method may be validated using a quasi-observational approach. Monte Carlo simulation (MCS) can be used to generate a synthetic catalog that is compatible with the properties of the seismicity of a site and the known relationship between ground motion, magnitude, and distance. The simulation can be repeated with a large number of trials to produce pseudo-observational data and reduces the problem to a simple counting of outcomes. Musson (2000) identified advantages include adaptability to different seismicity models, flexible handling of uncertainty, adaptability to risk analysis, and conceptually straightforward. On the other hand, disadvantages include non-unique results, and it is computationally slow. Monte Carlo simulation can also demonstrate that conventional PSHA does not produce unrealistic results and that the two models are mutually confirmatory.

Previous authors have adapted Monte Carlo simulation as their primary tool for seismic hazard assessment. Wang et al. (2015) conducted a Monte Carlo simulation of a well-studied earthquake catalog around Taipei, Taiwan. The statistics of magnitude and distance were determined, and Poisson distribution was assumed for earthquake frequency. Empirical relationships for predicting

ground motion based on local studies were used and treated as a random variable with equal probability to account for the epistemic uncertainty of the models. The PGA hazard curves plot shows that Taipei's current design PGA may not be conservative, similar to the results of a previous PSHA study. Similarly, the seismic zonation maps of Iran were developed using reliability methods to compute the exceedance probabilities of earthquake intensity measures (Rahimi et al., 2015). Probabilistic models for occurrence, location, and magnitude were used as input for the intensity models and were carried out for the nationwide seismic hazard analysis. The analysis was composed of 861 random variables and 57,615 model instances and was run using high-performance computers. Likewise, the insufficiency of seismological data has required Monte Carlo simulation to develop synthetic catalogs and determine the ground motion intensities in Southern Ghana (Osei et al., 2018). Seismic hazard curves and uniform hazard spectrum were generated for 2% and 10% probability of exceedance in 50 years. The study identified cities within Southern Ghana that are highly seismic and concluded that low-rise structures are exposed to high seismic risk. Comparably, Musson (2000) has performed MCS for low to moderate seismicity areas in the United Kingdom. The study showed that MCS is a safe alternative to PSHA and offers more flexibility in handling uncertainties in the input parameters.

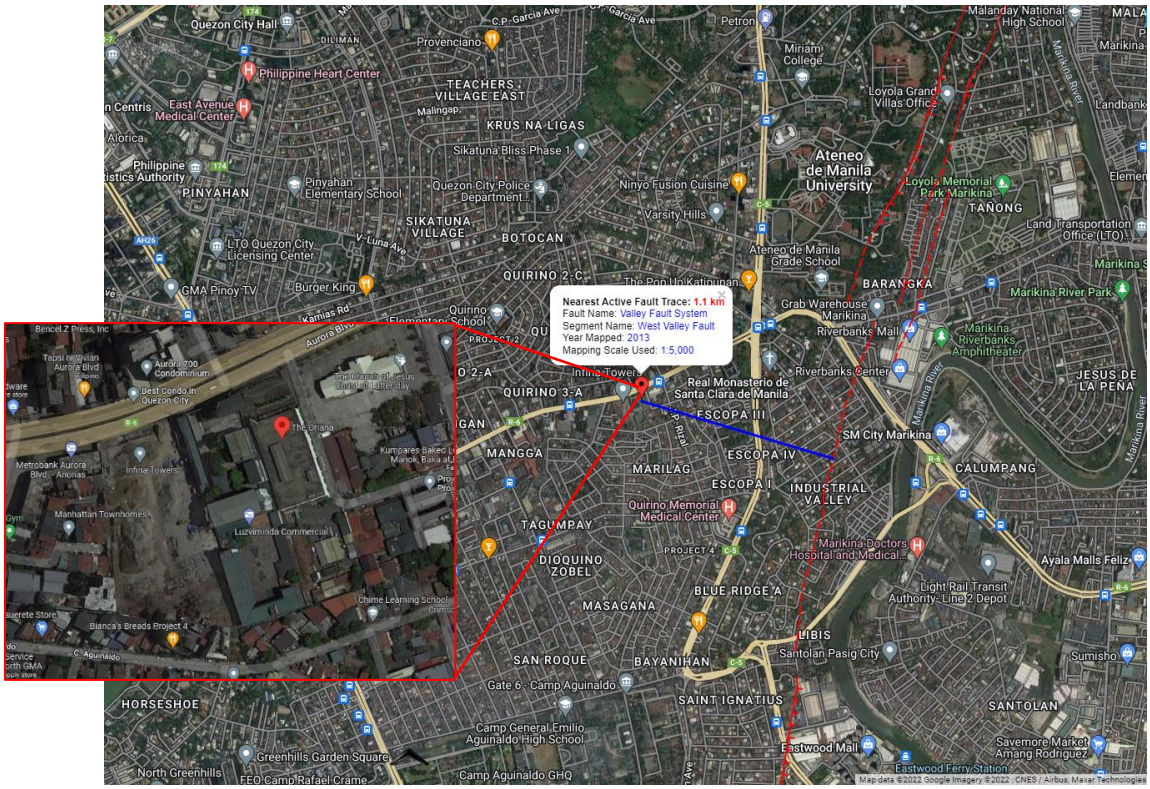

Figure 1. Project Site Location

The current study aims to validate the results of the conventional PSHA using reliability-based methods. Monte Carlo simulation is performed to estimate the seismic hazard of a residential building in Metro Manila and review its closeness with local technical references such as the Philippine Earthquake Model. Statistics of significant earthquakes are studied and will be used to simulate the magnitude, source-to-site distance, and focal depth to obtain synthetic catalogs at varying structural periods for up to five seconds. Randomization of variables was executed using

in-house algorithms in Excel. Seismic hazard curves and uniform hazard spectra are developed for several hazard levels.

II. STATISTICS OF MAJOR EARTHQUAKES AND GROUND MOTION PREDICTION EQUATIONS

The project site is located in Quezon City, Metro Manila, Philippines (Latitude: 14.628056ºN, Longitude: 121.068611ºE), and **Figure 1** shows the site location and its proximity to the West Valley Fault System. Geotechnical investigation reports that the underlying rock zone is presumed to be the Guadalupe Tuff Formation (GTF), and the soil engineer classifies the soil profile type as Type Sc (Vs = 360 to 760 m/s) and the seismic source type as Type B ($6.5 \leq M_w < 7.0$).

A historical earthquake catalog from the years 1900–2022 was obtained from the United States Geological Survey (USGS) database (*https://earthquake.usgs.gov/earthquakes/*). **Figure 2** shows the location of 808 major earthquakes ($M_w \geq 5.0$ and distance ≤ 400 km), and it is assumed that the data is declustered of foreshocks and aftershocks such that no dependent events exist in the catalog. The moment magnitude and distance criteria are similar to the conventional PSHA to obtain earthquake events of possible engineering significance.

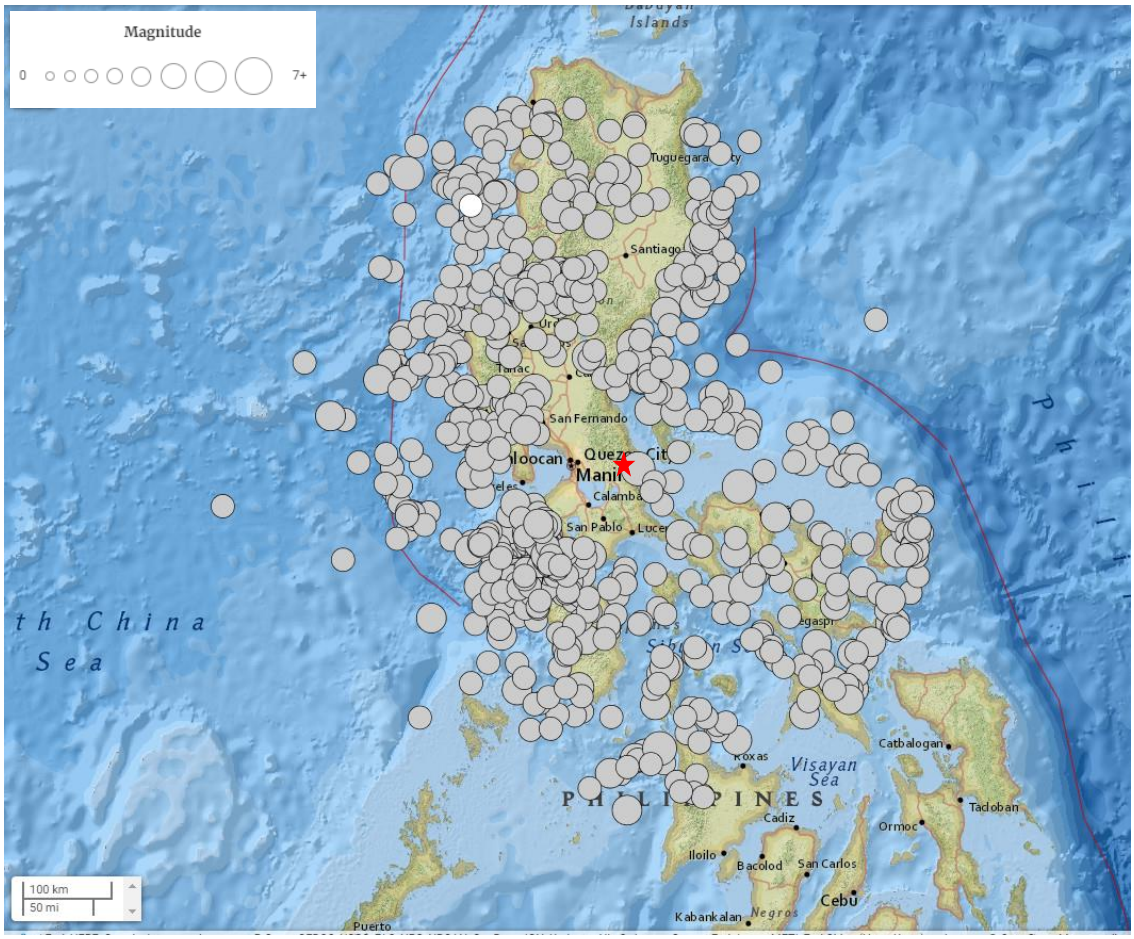

Figure 2. Seismicity Map ($M_w \geq 5.0$ and Distance ≤ 400 km)

The magnitude scales in the USGS catalog are defined in terms of surface-wave magnitude (M_s), body-wave magnitude (m_b), and moment magnitude (M_w). Ground motion models are usually defined in terms of the moment magnitude which requires the conversion of other magnitude types. Tang et al. (2016) performed General Orthogonal Regression (GOR) method to develop empirical equations for the conversion of surface-wave and body-wave magnitude to moment magnitude based on the earthquake catalog of Western China from the China Earthquake Data Center (CEDC). **Equations 1 and 2** lists the empirical formulas from 487 events used for calibration. In the absence of conversions based on local earthquake data, it is assumed that these equations are applicable in the current study.

$$M_w = -0.55 + 1.16m_b \tag{1}$$

$$M_w = 1.61 + 0.69M_S \tag{2}$$

Wang et al. (2014) verified the suitability of Poisson distribution in modeling the temporal probability of earthquakes based on 110-year-long earthquake data around Taiwan. Their study provided quantitative evidence of this hypothesis and its limits in seismic applications. It was concluded that design earthquakes with return periods longer than ten years follow the Poisson model and was suitable for earthquake engineering practices. **Equation 3** shows the probability

$$P(x) = \frac{e^{-v}v^x}{x!} \tag{3}$$

mass function (PMF) formula of Poisson distribution where v is the mean annual rate of earthquakes with $M_w \geq 5.0$ and x is the number of earthquakes per year. The mean annual rate based on the USGS catalog is 6.62 events per year and **Figure 3** shows the PMF of the Poisson model.

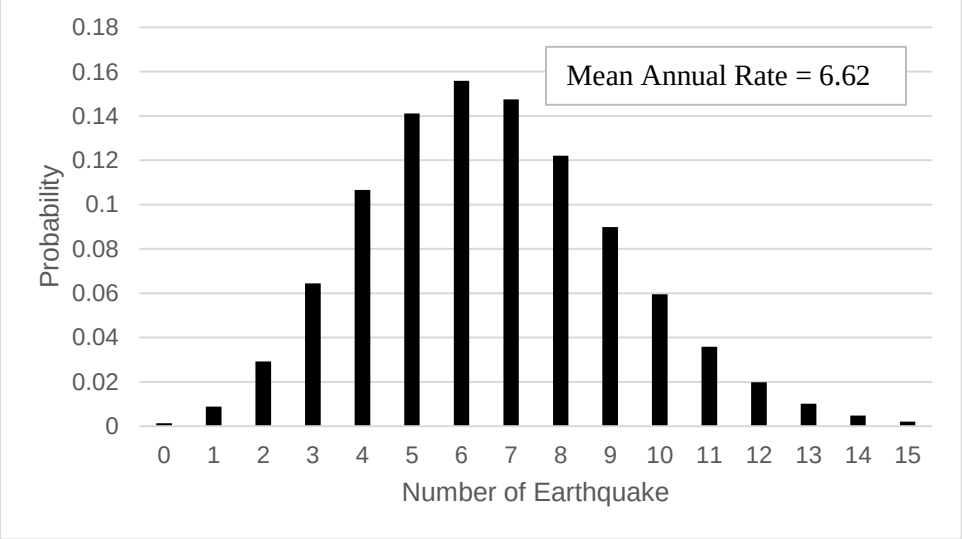

Figure 3. Probability Mass Function (Poisson Distribution) of Earthquake Frequency

Figures 4 and **5** show the frequency histogram of moment magnitude, source-to-site distance, and focal depth based on the earthquake catalog. The parameters of the histograms show that the mean magnitude and source-to-site distance are 5.6 and 213 km, respectively, while statistics of focal depth show that approximately one-third of the total events are shallow earthquakes. An earthquake is a shallow event if the focal depth is less than 30 km, which was adopted from the attenuation model that was used in this study (Kanno et al., 2006). The histograms can be converted to probability mass functions by dividing the frequency by the 808 events.

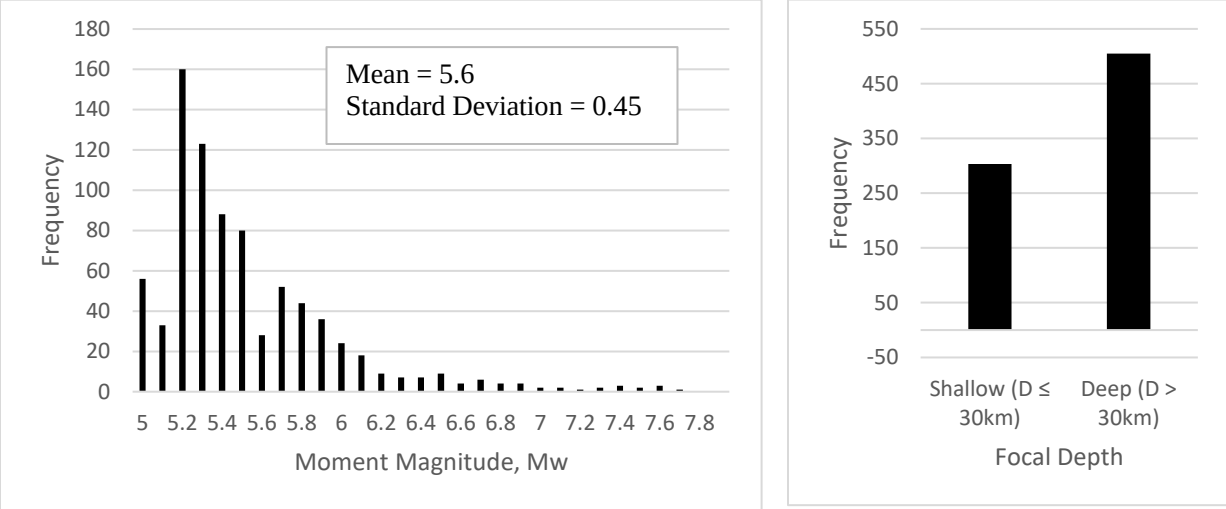

(a) **(b)**

Figure 4. Frequency Histogram: (a) Moment Magnitude (b) Focal Depth

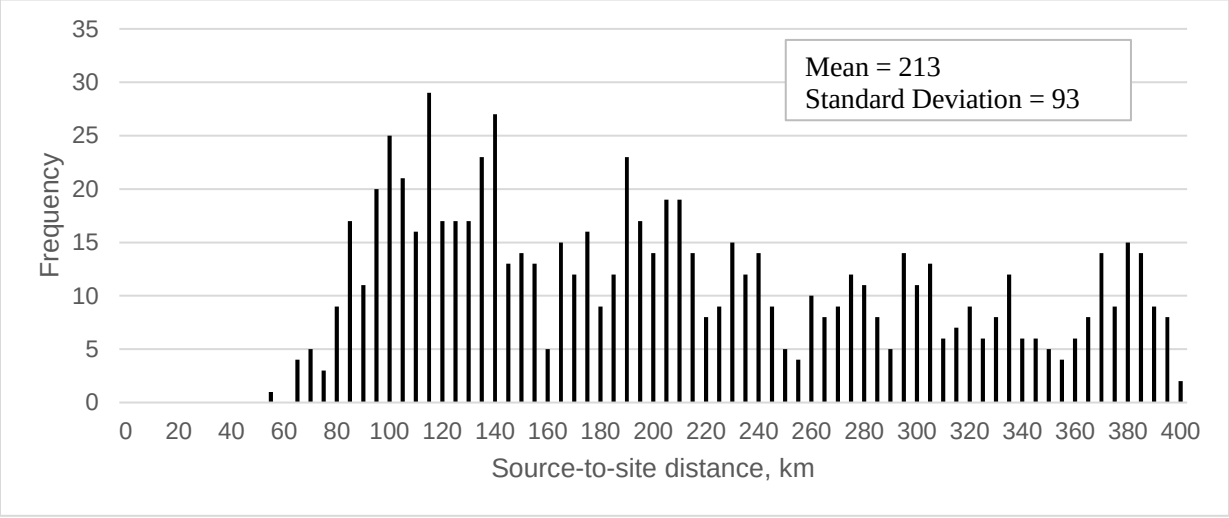

Figure 5. Frequency Histogram of Source-to-Site Distance

The R^2 value of the relationship was calculated to determine if there is any correlation between the moment magnitude and source-to-site distance by plotting the 808 major earthquakes as shown in

Figure 6. It can be observed that there is a low correlation between the two variables with an R^2 of 0.0026, and no transformation techniques are needed for the succeeding simulations.

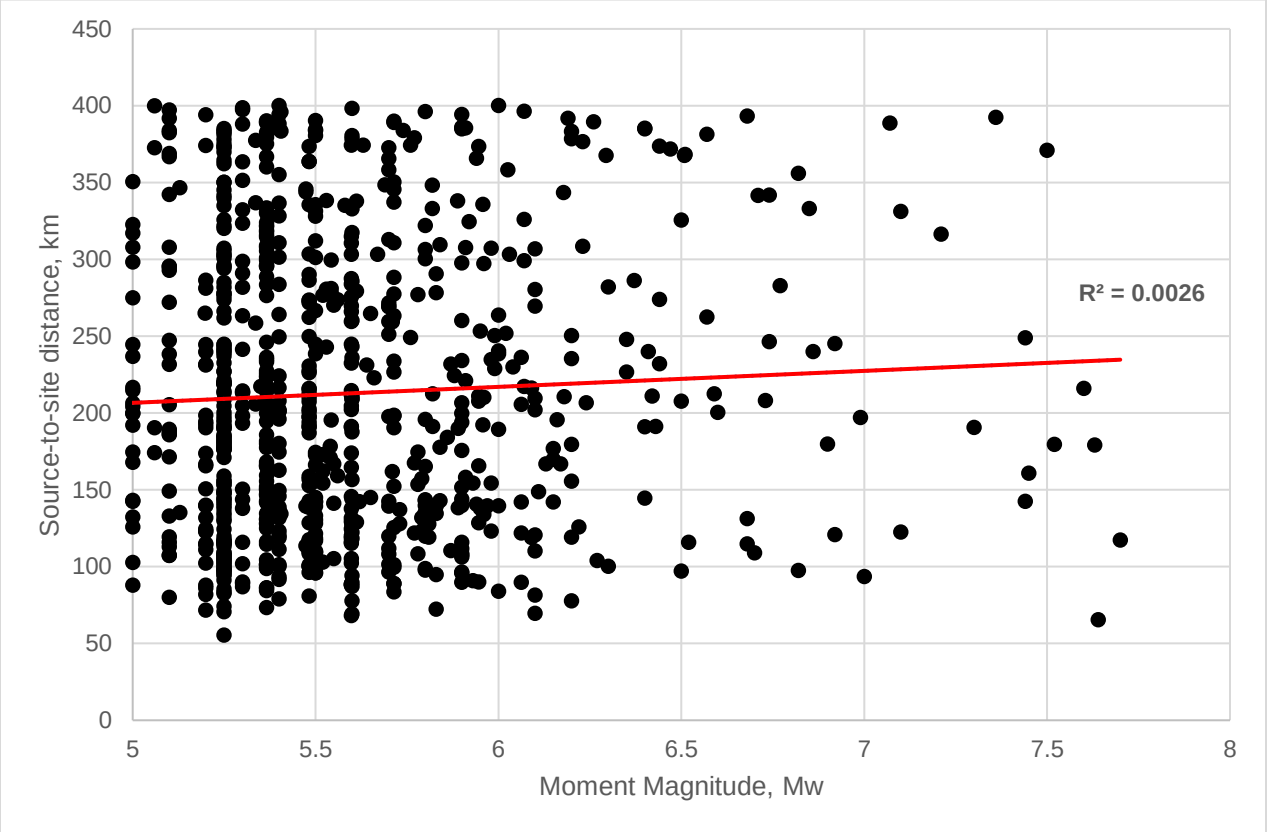

Figure 6. Correlation Plot of Source-to-Site Distance and Moment Magnitude

Kanno et al. (2006) developed attenuation models for peak ground acceleration (PGA), 5% damped response spectral acceleration (SA), and peak ground velocity (PGV). Regression models were developed from strong ground motion records of Japan from 1963 to 2003 and 12 earthquakes from other countries to improve the number of near-source data. Near-source data was weighted to improve the predictive capabilities of the model. The ground motion prediction equations (GMPE) were limited only to three parameters: moment magnitude (M_w), source-to-site distance (X), and focal depth (D), as shown in **Eq 4 and 5**,

$$\log pre = a_1 M_w + b_1 X - \log(X + d_1 * 10^{e_1 M_w}) + c_1 + \varepsilon_1 \qquad (D \leq 30\ km) \quad (4)$$

$$\log pre = a_2 M_w + b_2 X - \log(X) + c_2 + \varepsilon_2 \qquad (D > 30\ km) \quad (5)$$

where pre is the predicted peak ground acceleration (PGA) or 5% damped response spectral acceleration (SA), a_1,b_1,c_1,d_1,e_1,a_2,b_2,c_2 are regression coefficients, and ε_1 and ε_2 are the standard normal errors of the model shown in Table 1.

Table 1. Regression coefficients for shallow and deep event models

Period	Shallow Event						Deep Event			
(s)	a_1	b_1	c_1	d_1	e_1	ε_1	a_2	b_2	c_2	ε_2
PGA	0.56	-0.0031	0.26	0.0055	0.5	0.37	0.41	-0.0039	1.56	0.40
0.1	0.52	-0.0041	0.85	0.0073	0.5	0.40	0.10	-0.0043	2.12	0.46
0.15	0.52	-0.0038	0.89	0.0060	0.5	0.41	0.15	-0.0044	2.12	0.46
0.20	0.54	-0.0034	0.76	0.0053	0.5	0.40	0.20	-0.0042	2.02	0.44
0.30	0.56	-0.0026	0.51	0.0039	0.5	0.39	0.30	-0.0038	1.75	0.42
0.50	0.59	-0.0016	0.04	0.0022	0.5	0.41	0.50	-0.0030	1.19	0.40
1	0.71	-0.0009	-1.04	0.0021	0.5	0.41	1.00	-0.0022	0.08	0.41
1.5	0.77	-0.0009	-1.70	0.0017	0.5	0.40	1.50	-0.0020	-0.63	0.41
2	0.80	-0.0004	-2.08	0.0020	0.5	0.39	2.00	-0.0017	-1.12	0.40
3	0.86	-0.0002	-3.21	0.0045	0.5	0.38	4.00	-0.0016	-2.22	0.37

Table 2. Regression coefficients for the site correction term

Period (s)	p	q
PGA	-0.55	1.35
0.1	-0.32	0.78
0.15	-0.53	1.28
0.20	-0.68	1.65
0.30	-0.80	1.96
0.50	-0.91	2.25
1	-0.93	2.32
1.5	-0.85	2.12
2	-0.78	1.92
3	-0.62	1.54

Site correction factors are applied depending on the average shear-wave velocity of the site defined by the following:

$$AVSd = d \Big/ \sum_{i=1}^{n} ({}^{H_i}/_{V_{si}}) \tag{6}$$

$$G = p * logAVS30 + q \tag{7}$$

where n is the number of strata layers down to depth d, H_i denotes the thickness, V_{si} denotes the shear-wave velocity of the ith layer, G represents the correction term, and p and q are regression coefficients shown in Table 2. A value of 30 m is usually adopted for the depth. The correction term is then added to the initially calculated ground or spectral acceleration given as follows:

$$\log pre_g = \log pre + G \tag{8}$$

The same GMPEs were utilized to develop the Central Cebu Fault System (CCFS) PGA maps, which are potentially active faults (Mendoza et al, 2022).

III. SEISMIC HAZARD ASSESSMENT USING RELIABILITY-BASED METHODS

Reliability methods aim to measure structural safety by defining the reliability index or its complement, the probability of failure. Probabilistic theories capture uncertainties in the building

process and have been the rational basis for code developments (Nowak, 2013). These methods were developed to compute the probability of rare events which are suited to hazard analysis applications.

Monte Carlo simulation can be used to generate synthetic earthquake catalogs via random sampling of observed seismicity. The expected ground motion is estimated from the synthetic catalog and empirical attenuation models, from which seismic hazard is derived (Weatherhill and Burton, 2010). Random variables, such as moment magnitude and source-to-site distance, are simulated by generating uniformly distributed numbers between 0 and 1. Applicability of reliability methods are extended to seismic hazard assessment by defining the limit state function as:

$$g(x) = I_o - I(x) \tag{9}$$

where I_o is the spectral acceleration of interest, and I(x) is the spectral acceleration for a given seismic event from the synthetic catalog. The probability of failure (P_f) corresponds to the number of simulations where g(x) is negative. In seismic hazard analysis, the probability of failure is the annual frequency of exceedance, and the pair (I_o, P_f) is a point on the hazard curve (Rahimi et al., 2015). **Figure 7** illustrates the flow diagram corresponding to the Monte Carlo simulation of 100,000 trials at different structural periods adapted from the framework of Wang et al. (2015). A sample simulation of five trials is shown in the appendix.

From the observation of the results of a large number of simulations of several catalogs, probabilities are obtained by counting the number of simulations exceeding a specific value. 100,000 simulations of 100 years of seismicity give an equivalent 10,000,000 years of data (Musson, 2000). In this study, the number of trials used is 100,000 to obtain seismic hazard curves up to a 10,000-year return period.

Seismic hazard curves are developed for PGA and SA for periods up to five seconds based on an idealized shear wave velocity (V_{S30}) of 760 m/s. The uniform hazard spectrum for a return period of 43 (50% in 30 years), 475 (10% in 50 years), and 2475 (2% in 50 years) years are compared with the results of conventional PSHA performed by Fugro (2020). Peak ground acceleration (PGA), Short-period spectral acceleration (S_s), and spectral acceleration for a period of 1s (S_1) are also compared with the recommendations from the Philippine Earthquake Model (PEM) for a 500-year return period on the V_{S30} site model.

IV. DATA AND RESULTS

Figure 8 shows the seismic hazard curves for PGA and SA up to five seconds from the 100,000 trials for each structural period. **Figure 9** shows the uniform hazard spectra comparison of conventional PSHA and MCS-based PSHA. For Service-level earthquake (43-year return period), the MCS-based approach overpredicts the spectral acceleration at a period range of 0 to 0.3s but has a good correlation at a period range of 0.3 to 5s. On the other hand, Design Earthquake (475-year return period) and Maximum Considered Earthquake (2475-year return period) from MCS overestimate the spectral acceleration for periods below 0.15s while underestimating the spectral acceleration at a period range of 0.15 to 5s. The MCE_R spectral acceleration from conventional

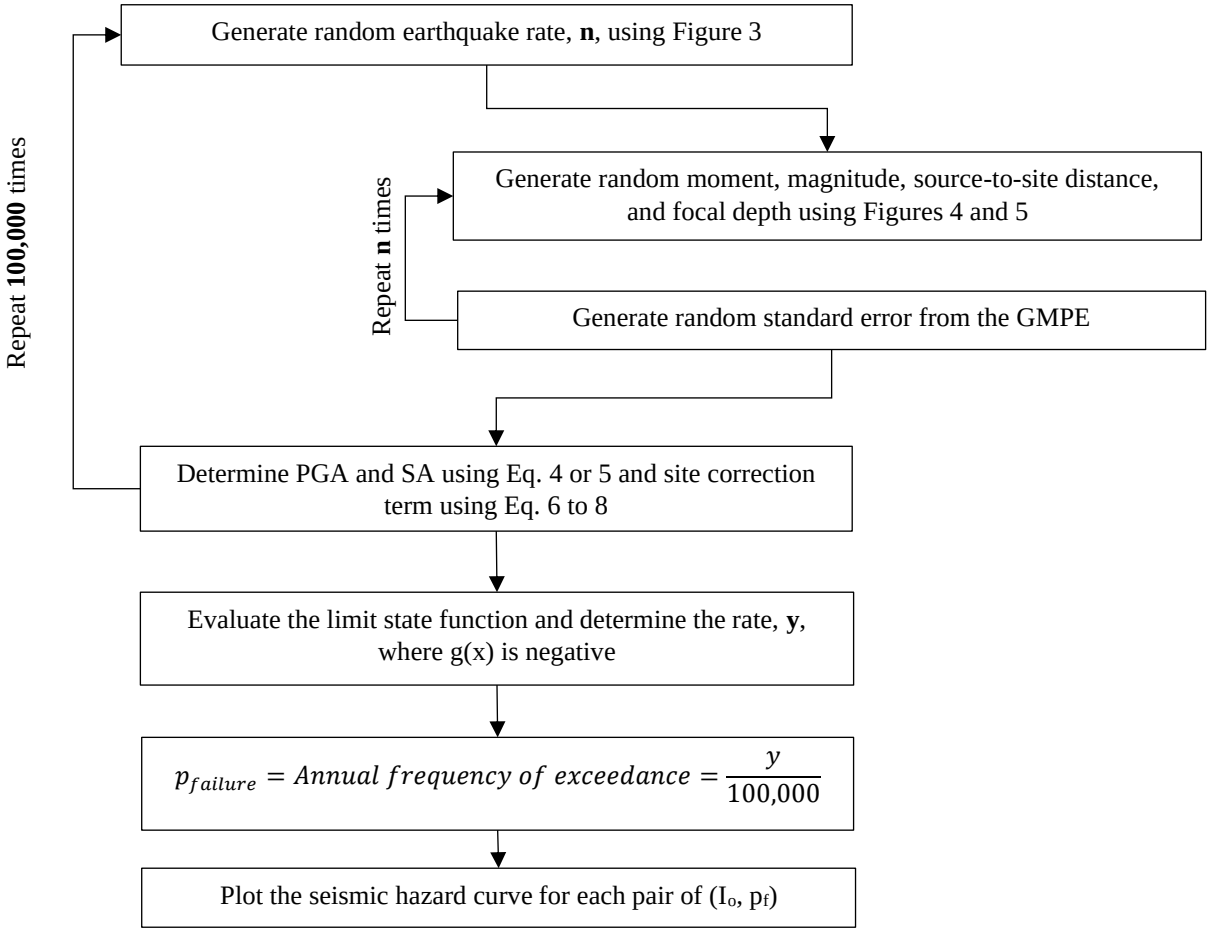

Figure 7. Flowchart of Monte Carlo Simulation of Seismic Hazard Assessment

PSHA peaks at 2.31g while the MCS-based approach peaks at 2.70g. **Table 3** presents the root mean square error (RMSE) for each plot of the return period. It can be inferred that the error between the two methods increases at higher return periods.

Table 3. Root Mean Square Error of Uniform Hazard Spectra

Return Period	RMSE
43 (SLE)	0.0846
475 (DE)	0.2382
2475 (MCE_R)	0.3006

The difference in the results of the two studies may be attributed to the GMPEs used in the analysis. GMPEs used in the conventional PSHA account for the project site's rupture mechanism and regional geology. Next-generation attenuation (NGA) West-2 GMPEs for shallow crustal and subduction sources were modeled using recent attenuation equations such as Campbell and Bozorgnia (2014) and Abrahamson et al. (2015). Moreover, near-source effects were also considered in the conventional method resulting in an overall increase in the average ground motion. On the other hand, the GMPE for MCS introduced a weighting scheme into the base model to increase the statistical power of near-source data (Kanno et al., 2006).

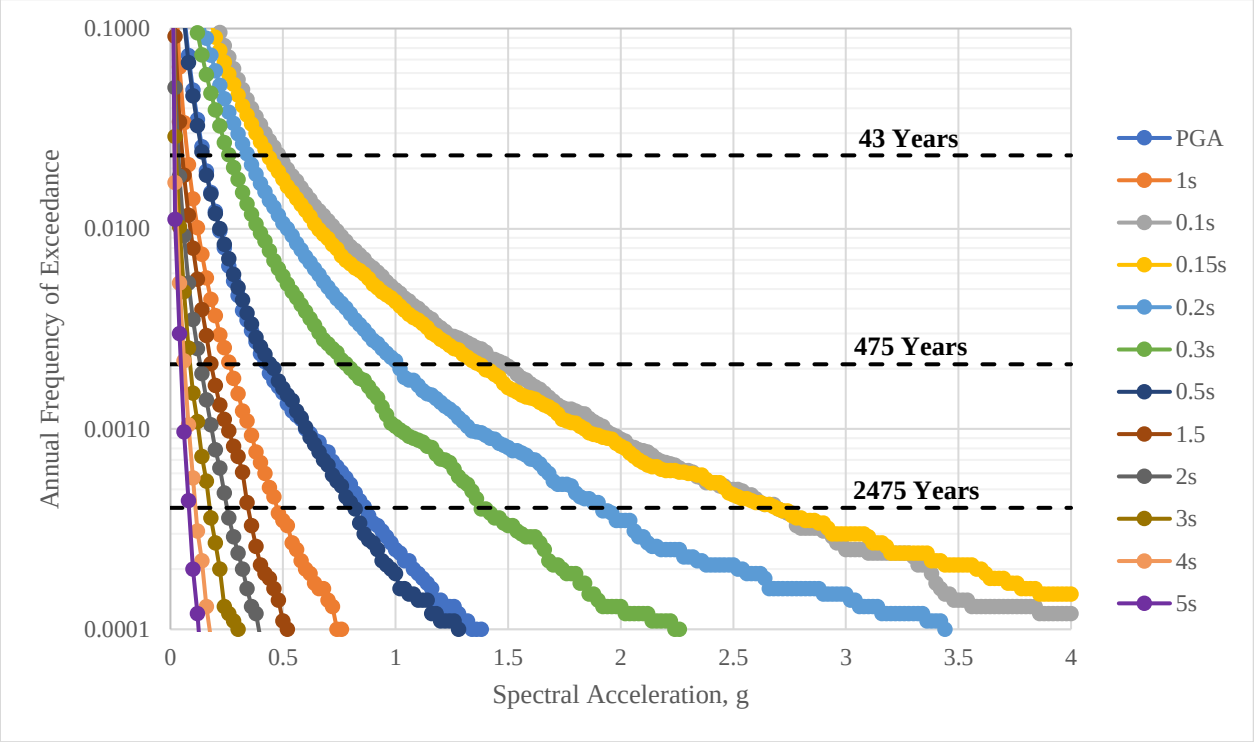

Figure 8. MCS Annual Hazard Curves for Different Structural Periods (V_{S30} = 760 m/s)

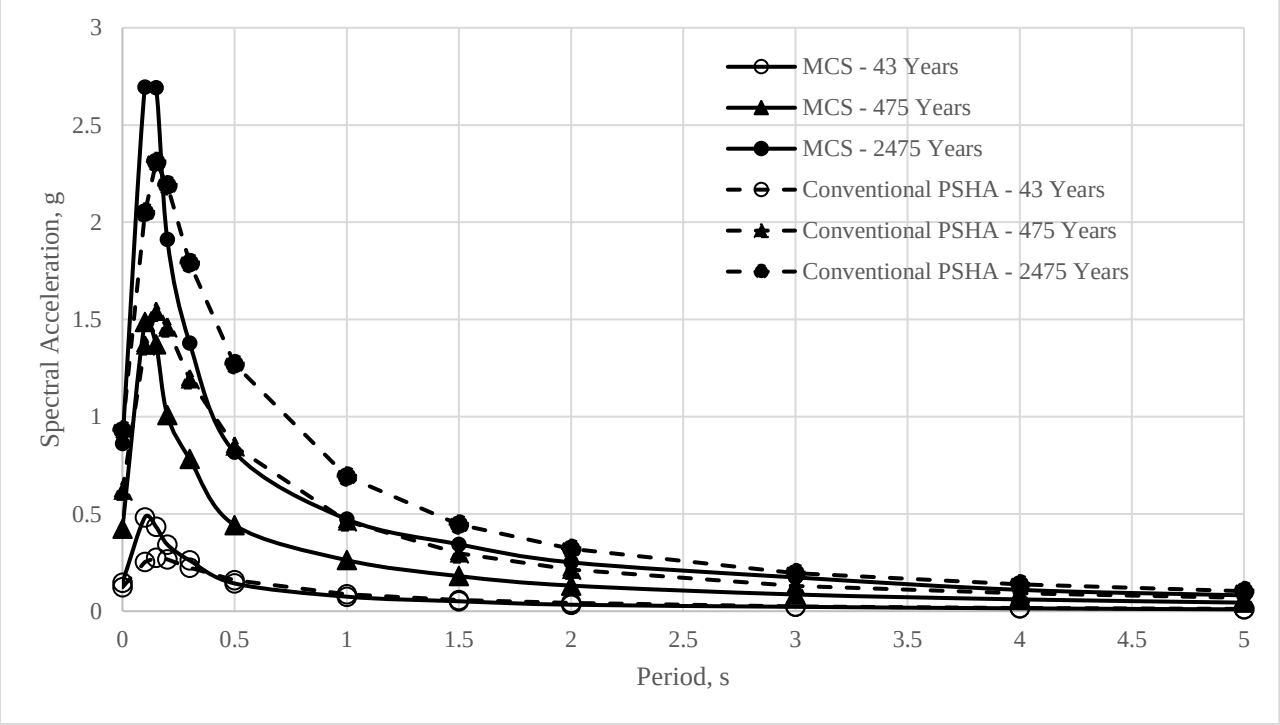

Figure 9. Site-specific Uniform Hazard Spectra (V_{S30} = 760 m/s)

Table 4 gives the comparison of PGA, S_s, and S_1 values obtained from MCS with the Philippine Earthquake Model for a 500-year return period earthquake. PGA, S_s, and S_1 are close, if not within, the recommended acceleration range of PEM. Comparing the Monte Carlo simulation results with conventional PSHA by Fugro and the Philippine Earthquake Model shows that MCS can be an alternative approach to verify the conventional PSHA since the two methods have relatively similar results.

Table 4. Comparison of Ground Acceleration of PEM and MCS

Ground Motion (500-year Return Period)	Philippine Earthquake Model	Monte Carlo Simulation
PGA	0.40 – 0.45	0.432
S_s	0.95 – 1.00	1.02
S_1	0.20	0.268

V. CONCLUSION

Statistics of major earthquakes ($M_w \geq 5.0$ and distance ≤ 400 km) around the project site located in Metro Manila were determined from a 122-year catalog obtained from USGS. The study shows that the mean annual earthquake rate is 6.62, with the mean and standard deviation of the moment magnitude equal to 5.6 and 0.45, respectively. Similarly, the mean and standard deviation of source-to-site distance is 213 km and 93 km, and there is approximately a 33% chance that the earthquake will be a shallow event.

Earthquake statistics and ground motion prediction models can be used to conduct Monte Carlo simulations as an alternative approach to the conventional PSHA. A comparison of uniform hazard spectra shows that MCS overestimates the spectral accelerations at a period range of 0 to 0.15s while underestimating at a period range of 0.15 to 5s. The root mean square errors show that the deviation of the two methods increases at higher return periods. Furthermore, a comparison of MCS with the Philippine Earthquake Model shows that the PGA, S_s, and S_1 have relatively similar values. This study shows that reliability-based methods can validate the results of conventional PSHA since the two methods are from entirely different routes and are mutually confirmatory.

APPENDIX

Table A1 shows a demonstration of the algorithm of Monte Carlo simulation (**Figure 7**) using the earthquake statistics developed in the study. Columns 2 to 6 were obtained from the generation of random numbers using the rand() function of Excel. The ground motion intensity is calculated using the appropriate equation depending on the focal depth and regression coefficients from **Table 1**. The modified ground motion intensity is determined by applying the correction term for V_{S30} of 760 m/s, as shown in column 10. Ground motions are usually in terms of gravitational acceleration, g, and the final ground motions are listed in column 11.

The ground motions (I(x)) from the simulation wherein a spectral acceleration of interest (I_o) say, 0.01g, has been exceeded are shown in bold fonts. These PGA values would result in a negative g(x) in the limit state function. To determine the annual rate of exceedance, the number of instances where g(x) is negative is divided by the number of trials. The annual rate of exceedance of 0.01g using a sample size of five would be two per year since the total number of instances is ten and the total number of trials is five.

Table A1. MCS-based Seismic Hazard Assessment with Five Trials for PGA

Trial	Earthquake Rate, n	Mw	Distance (km)	Focal Depth	Error	log PGA	G	log PGA_G	PGA, (cm/s^2)	PGA* (g)
1	10	5.2	115	Deep	0.392	1.575	-0.234	1.340	21.887	**0.022**
		5.4	130	Shallow	0.186	0.944	-0.234	0.710	5.125	0.005
		5.2	65	Shallow	-0.161	0.982	-0.234	0.747	5.590	0.006
		5.5	320	Shallow	-0.419	-0.580	-0.234	-0.815	0.153	0.000
		5.3	120	Shallow	0.236	1.004	-0.234	0.770	5.887	0.006
		7.4	210	Deep	0.070	1.523	-0.234	1.288	19.414	**0.020**
		5.3	125	Deep	0.680	1.829	-0.234	1.595	39.319	**0.040**
		5.2	90	Deep	-0.652	0.734	-0.234	0.500	3.163	0.003
		7	115	Deep	-0.075	1.846	-0.234	1.611	40.842	**0.042**
		5.3	190	Shallow	0.686	1.041	-0.234	0.806	6.404	0.007
2	6	5.7	340	Shallow	0.445	0.306	-0.234	0.072	1.180	0.001
		5.3	205	Shallow	0.005	0.280	-0.234	0.046	1.111	0.001
		5.3	260	Deep	-0.098	0.206	-0.234	-0.029	0.936	0.001
		5.2	315	Deep	0.028	-0.007	-0.234	-0.241	0.574	0.001
		5.2	105	Shallow	-0.340	0.476	-0.234	0.242	1.746	0.002
		5.5	230	Shallow	0.105	0.364	-0.234	0.130	1.349	0.001
3	3	7.6	315	Deep	0.190	1.139	-0.234	0.905	8.030	0.008
		5.1	215	Shallow	-0.522	-0.409	-0.234	-0.644	0.227	0.000
		5.2	215	Deep	-0.517	0.004	-0.234	-0.230	0.589	0.001
4	3	6.4	230	Deep	0.424	1.349	-0.234	1.115	13.032	**0.013**
		5.2	385	Shallow	-0.186	-0.796	-0.234	-1.030	0.093	0.000
		5.4	140	Deep	-0.241	0.841	-0.234	0.607	4.044	0.004
5	9	5.3	325	Shallow	-0.226	-0.521	-0.234	-0.756	0.176	0.000
		5.3	95	Deep	0.083	1.468	-0.234	1.234	17.122	**0.017**
		5.9	140	Deep	0.030	1.317	-0.234	1.082	12.081	**0.012**
		5.2	350	Deep	-0.307	-0.524	-0.234	-0.759	0.174	0.000
		5.4	80	Deep	0.066	1.625	-0.234	1.390	24.562	**0.025**
		5.3	195	Deep	0.164	0.847	-0.234	0.612	4.093	0.004
		6.5	115	Deep	-0.318	1.397	-0.234	1.163	14.550	**0.015**
		5.9	125	Deep	-0.068	1.327	-0.234	1.092	12.371	**0.013**
		7.2	345	Deep	-0.129	0.500	-0.234	0.265	1.842	0.002

*g = 980.665 cm/s^2

REFERENCES

Baker, Jack W. (2015) Introduction to Probabilistic Seismic Hazard Analysis. White Paper Version *2.1*, 77 pp.

Eskandarinejad, A., Zafarani, H., & Jahanandish, M. (2018). Comparison of conventional and Monte Carlo simulation-based probabilistic seismic hazard analyses for Shiraz city, Southern Iran. *Journal of Seismology*, *22*(6), 1629–1643. https://doi.org/10.1007/s10950-018-9790-5

Fugro USA Land, Inc. (2020). Probabilistic Seismic Hazard Assessment: Aurora Property. Unpublished internal company document.

Kanno, T. (2006). A new attenuation relation for strong ground motion in Japan based on recorded data. *Bulletin of the Seismological Society of America*, *96*(3), 879–897. https://doi.org/10.1785/0120050138

Mendoza, R. B., Ramos, N., & Dimalanta, C. (2022). High-resolution peak ground acceleration modeling using geographic information systems: A case study of the potentially active Central Cebu Fault System, Philippines. *Journal of Asian Earth Sciences: X*, *7*, 100097. https://doi.org/10.1016/j.jaesx.2022.100097

Musson, R. M. (2012). Psha validated by quasi observational means. *Seismological Research Letters*, *83*(1), 130–134. https://doi.org/10.1785/gssrl.83.1.130

Musson, R. M. (2000). The use of Monte Carlo simulations for Seismic Hazard Assessment in the U.K. *Annals of Geophysics*, *43*(1). https://doi.org/10.4401/ag-3617

Nowak, A. S., & Collins, K. R. (2013). *Reliability of structures*. CRC Press/Taylor & Francis Group.

Osei, J. B., Adom-Asamoah, M., Awadallah Ahmed, A. A., & Antwi, E. B. (2018). Monte Carlo based seismic hazard model for Southern Ghana. *Civil Engineering Journal*, *4*(7), 1510. https://doi.org/10.28991/cej-0309191

Philippine Institute of Volcanology and Seismology (2017). The Philippine Earthquake Model. Diliman, Quezon City. DOST-PHIVOLCS

Philippine Institute of Volcanology and Seismology (2021). Spectral Acceleration Maps of the Philippines (SAM PH). Diliman, Quezon City. DOST-PHIVOLCS

Rahimi, H., Mahsuli, M., Bakhsi, A. (2015). Reliability-based Seismic Hazard Analysis. In *12th International Conference on Applications of Statistics and Probability in Civil Engineering.* Retrieved June 2022, from https://open.library.ubc.ca

Tang, C. C., Zhu, L., & Huang, R. (2016). Empirical*m*w–*m*l,*m*b, and*m*sconversions in western China. *Bulletin of the Seismological Society of America*, *106*(6), 2614–2623. https://doi.org/10.1785/0120160148

Wang, J. P., Huang, D., Chang, S.-C., & Wu, Y.-M. (2014). New evidence and perspective to the Poisson process and earthquake temporal distribution from 55,000 events around Taiwan since 1900. *Natural Hazards Review, 15*(1), 38–47. https://doi.org/10.1061/(asce)nh.1527-6996.0000110

Wang, J. P., Wu, Y.-M., & Huang, D. (2015). Major earthquakes around Taipei and a seismic hazard assessment with Monte Carlo Simulation. *Natural Hazards Review*, *16*(4). https://doi.org/10.1061/(asce)nh.1527-6996.0000176

Weatherill, G., & Burton, P. W. (2010). An alternative approach to probabilistic seismic hazard analysis in the Aegean Region using Monte Carlo Simulation. *Tectonophysics*, *492*(1-4), 253–278. https://doi.org/10.1016/j.tecto.2010.06.022